Cancer Chemotherapy and Pharmacology (2026) 96:60
https://doi.org/10.1007/s00280-026-04907-8

ORIGINAL ARTICLE

Autophagy impairs the sensitivity of Ewing sarcoma cells to PARP inhibitors

Julia Clausen[1,2] · Daniela Kocher[1,2,3] · Hauke M. Schadwinkel[1,2,4] · Sabine Becker[1,2,3] · Till Milde[1,3,5,6] · James F. Beck[1] · Jürgen Sonnemann[1,2,3]

Received: 16 December 2025 / Accepted: 11 May 2026
© The Author(s) 2026

Abstract

Purpose PARP inhibitors (PARPi) proved effective in Ewing sarcoma cells in preclinical studies. In clinical evaluation, however, the PARPi olaparib failed to elicit substantial responses, suggesting an unknown mechanism of resistance to PARPi in Ewing sarcoma. Since autophagy has been identified as a PARPi resistance mechanism in other tumours, this study aimed at exploring the impact of autophagy on PARPi effectiveness in Ewing sarcoma cells.

Methods Effects of the PARPi olaparib and veliparib were assessed by flow cytometry in the Ewing sarcoma cell lines WE-68 and SK-ES-1. Autophagy levels were determined using the autophagosome tracer dye Cyto-ID, and cytotoxic effects were determined by the analysis of cell death and loss of mitochondrial membrane potential. Cyto-ID was used to separate cell populations into subpopulations with low, medium and high autophagy by flow cytometric cell sorting.

Results Olaparib and veliparib induced autophagy and cell death in parallel in WE-68 and SK-ES-1 cells. Induction of autophagy and cell death occurred at the same concentrations of both PARPi in both cell lines. Analysis of cells sorted according to autophagy levels revealed a clear association between PARPi effectiveness and autophagy level. The subpopulation of Ewing sarcoma cells with high autophagy responded significantly less to PARPi with cell death than the subpopulation with low autophagy.

Conclusion This study demonstrates that autophagy affects the anticancer activity of PARPi in Ewing sarcoma cells.

Keywords Ewing sarcoma · PARP · Olaparib · Celiparib · Autophagy · Cyto-ID · Cell sorting

✉ Hauke M. Schadwinkel
h.schadwinkel@uke.de

Julia Clausen
julia.schneekloth@outlook.de

Daniela Kocher
Daniela.Kocher@med.uni-jena.de

Sabine Becker
Sabine.Becker@med.uni-jena.de

Till Milde
Till.Milde@med.uni-jena.de

James F. Beck
James.Beck@gmx.de

Jürgen Sonnemann
Juergen.Sonnemann59@gmail.com

[1] Department of Paediatric and Adolescent Medicine, Jena University Hospital, Friedrich Schiller University Jena, Jena, Germany

[2] Research Centre Lobeda, Jena University Hospital, Friedrich Schiller University Jena, Jena, Germany

[3] Comprehensive Cancer Centre Central Germany (CCCG), Jena, Germany

[4] Department of Ophthalmology, UKE Hamburg, Hamburg, Germany

[5] Hopp Children's Cancer Center Heidelberg (KiTZ), Heidelberg, Germany

[6] Clinical Cooperation Unit Pediatric Oncology, German Cancer Research Center Heidelberg (DKFZ), Heidelberg, Germany

Published online: 30 May 2026

Abbreviations

Aut^{HI}	High autophagy
Aut^{LO}	Low autophagy
Aut^{ME}	Medium autophagy
CQ	Chloroquine
$DiIC_1(5)$	1,1',3,3,3',3'-hexamethylindodicarbocyanine iodide
ES	Ewing sarcoma
FSC-A	Forward light scatter area
FSC-H	Forward light scatter height
FSC-W	Forward light scatter width
IFM	Indicator-free medium
PARP	Poly(ADP-ribose)-polymerase
PARPi	PARP inhibitor
PI	Propidium iodide
SSC-A	Sideward light scatter area
SSC-H	Sideward light scatter height
SSC-W	Sideward light scatter width

Introduction

Ewing sarcoma (ES) is a highly aggressive cancer of bone and soft tissue, primarily affecting children, adolescents and young adults [1, 2]. Less than 10% of patients with ES survived before the introduction of chemotherapy. With the development of intensive multimodality therapy, consisting of multidrug cytotoxic chemotherapy along with surgery and/or radiotherapy, the prognosis improved steadily over the last decades of the twentieth century, leading to a five-year survival of around 70% overall in high-income countries [3]. However, the prognosis has improved only slightly since the turn of the century despite continuous attempts at treatment intensification [4]. This suggests that the chemotherapy protocols have been optimised to their limits and emphasises the need for new therapeutic approaches.

ES is caused by a pathognomonic chromosomal translocation in which an FET family gene fuses with an ETS family gene [1, 2]. In about 85% of cases, this translocation results in the EWSR1::FLI1 gene fusion encoding the chimeric oncoprotein EWS::FLI1 [5]. The latter is responsible for the initiation and progression of ES by acting mainly as a neomorphic transcription factor. Although EWS::FLI1 thus is a logical candidate target in ES, its direct targeting is challenging due to its function as a transcription factor [6, 7], and has had limited clinical success to date [8].

However, EWS::FLI1-mediated downstream aberrations may serve as druggable vulnerabilities [6, 7]. For example, EWS::FLI1 promotes R-loop accumulation and elevates replication stress, resulting in a 'BRCAness' phenotype [9]. ES is therefore particularly susceptible to agents that target proteins involved in replication stress and the DNA damage response [10–12]. Accordingly, inhibitors of DNA repair-associated proteins such as ATR, CDC7 or DNA-PK have demonstrated effectiveness against ES in preclinical studies [13–18].

The inhibition of poly(ADP-ribose)-polymerase (PARP) is considered to have particular potential in ES therapy [19, 20]. EWS::FLI1 drives PARP expression, which further increases EWS::FLI1-induced transcription in a positive feedback loop [21]. In line with this observation, ES cells were found to be as sensitive to PARP inhibitor (PARPi) treatment as BRCA1-deficient cancer cells, and EWS::FLI1 was identified as a biomarker for PARPi responsiveness [22]. However, although the PARPi olaparib was highly effective against ES in vitro [21–23], a phase II trial of olaparib in ES patients failed to deliver meaningful clinical benefits [24]. This indicates that PARPi monotherapy is not sufficient to achieve an objective response in ES [19].

Various approaches are being pursued to overcome the lack of response to PARPi in different cancer types [25–27]. In in vitro models of ES, PARPi cooperated with different cytotoxic agents to elicit cell death [28–30]. Phase I and II ES trials of PARPi in combination with either of the cytotoxic drugs irinotecan or temozolomide demonstrated limited antitumour activity [31, 32], while a phase I trial of the triplet combination with irinotecan and temozolomide suggested clinical benefit [33]. Yet haematological toxicity limited the clinical feasibility of dose escalation, implying that PARPi should rather be combined with non-cytotoxic agents [34]. A deeper understanding of the factors mediating PARPi resistance could therefore lead to superior combination partners that may benefit ES patients.

Autophagy is a fundamental cytoprotective activity [35] that has emerged as an important actionable resistance mechanism to chemotherapy and targeted therapy [36, 37], including PARPi [38]. PARPi have been found to induce autophagy, and cotreatment with autophagy inhibitors has been shown to enhance PARPi sensitivity in ovarian, hepatocellular, breast and prostate cancer cells [39–42]. Autophagy may also be a useful therapeutic target in ES, although its role is ambiguous, as it can function both as tumour promoter and suppressor [43]. The relevance of autophagy for the effectiveness of PARPi in ES, however, has not yet been examined. To explore this matter, we have used a flow-cytometric cell sorting procedure that separates ES cell populations into fractions with low, medium and high autophagy (hereafter referred to as Aut^{LO}, Aut^{ME} and Aut^{HI}, respectively). We found that the Aut^{HI} fraction was less sensitive to the PARPi olaparib and veliparib than the Aut^{LO} fraction, indicating that autophagy indeed is a resistance mechanism to PARPi in ES.

Materials and methods

Cell culture

WE-68 (RRID: CVCL_9717) cells were kindly provided by Dr F. van Valen (Münster, Germany), and SK-ES-1 (RRID: CVCL_0627) cells were purchased from the DSMZ (Braunschweig, Germany). Cells were cultured in RPMI 1640 medium (Capricorn Scientific, Ebsdorfergrund, Germany), supplemented with 10% foetal calf serum (Capricorn Scientific), 100 units/ml penicillin G sodium and 100 µg/ml streptomycin sulphate (Lonza, Basel, Switzerland). Cells were maintained throughout in rat-tail collagen-coated (5 µg/cm^2; Merck, Darmstadt, Germany) cell culture vessels in a humidified atmosphere containing 5% CO_2 at 37 °C and regularly passaged at a confluence of 90%. Mycoplasma contamination was routinely checked with the qPCR Mycoplasma Test Kit from Applichem (Darmstadt, Germany).

Treatment of cells

Cells were seeded in 12-well tissue culture plates at a density of 150,000 cells/well. Twenty-four hours after seeding, cells were treated with the PARPi olaparib (0.1–4 µM) or veliparib (2–80 µM; Biomol, Hamburg, Germany) for 48 h. Olaparib and veliparib were dissolved in DMSO to prepare stock solutions and stored at −80 °C. In the experiments shown in Fig. 2, cells were treated with PARPi for 24 h before treatment with the autophagy inhibitor chloroquine (CQ; 25 µM; Enzo Life Sciences, Lörrach, Germany) for 6–24 h. CQ was dissolved in PBS to prepare a stock solution and stored at 4 °C. In the cell sorting experiments, cells were seeded 2 h after sorting at a density of 100,000 cells/well and treated with PARPi for 48 h.

Flow-cytometric analysis of cell death

Cell death was analysed by assessing the cell membrane integrity by flow-cytometric analysis of propidium iodide (PI; Sigma Aldrich) uptake. After harvesting, cells were incubated in 2 µg/ml PI in PBS at 4 °C immediately before analysis. 10,000 cells per sample were analysed on a BD (Heidelberg, Germany) FACSCanto II using BD FACSDiva software. Data were gated based on forward light scatter area (FSC-A) versus sideward light scatter area (SSC-A) to exclude debris and doublets.

Flow-cytometric analysis of autophagy

Cells were stained with Cyto-ID (Enzo Life Sciences) according to the manufacturer's recommendations. In brief, cells were washed with indicator-free medium (IFM), consisting of phenol red-free RPMI 1640 medium (Capricorn Scientific) containing 5% FCS and 2 mM L-glutamine (Lonza), and incubated in Cyto-ID at a dilution of 1:1000 in IFM for 30 min at 37 °C. After washing and resuspension in IFM, PI was added to a final concentration of 2 µg/ml immediately before analysis. 10,000 cells per sample were analysed on a FACSCanto II using FACSDiva software. Data were gated based on FSC-A versus SSC-A to exclude debris and doublets and further gated on PI-negative populations to exclude dead cells.

Flow-cytometric analysis of mitochondrial transmembrane potential ($\Delta\psi_m$) dissipation

The loss of $\Delta\psi_m$ was analysed by determining 1,1',3,3,3',3'-hexamethylindodicarbocyanine iodide ($DiIC_1(5)$; Thermo Fisher Scientific, Dreieich, Germany) staining of mitochondria. Before harvesting, cells were incubated with 50 nM $DiIC_1(5)$ for 45 min at 37 °C in the dark. 10,000 cells per sample were analysed on a BD FACS Canto II using BD FACSDiva software. Data were gated based on FSC-A versus SSC-A to exclude debris and doublets.

Flow-cytometric cell sorting based on Cyto-ID staining

The method for sorting ES cells based on Cyto-ID staining was adapted from our recently developed method for sorting leukaemia cells based on Cyto-ID staining [44]. Accordingly, 1×10^7 cells were stained with Cyto-ID as described, resuspended in 1 ml IFM, filtered through 35-µm mesh and incubated with 1 µM Sytox Blue (Thermo Fisher Scientific) immediately before sorting. Cells were sorted into three subpopulations of approximately equal number according to the Cyto-ID fluorescence intensity, i.e., into Aut^{LO}, Aut^{ME} and Aut^{HI} populations. To minimise the starvation period during the sorting procedure, the collection tubes were prefilled with 1 ml of complete growth medium or IFM, depending on the subsequent analysis. Sorting was done on a BD FACSAria Fusion at 45 psi using an 85 µM nozzle at 4 °C. Debris and aggregates were excluded from sorting using a sequential gating strategy relying on FSC-A versus SSC-A followed by FSC height (FSC-H) versus FSC width (FSC-W) and SSC height (SSC-H) versus SSC width (SSC-W) (see Fig. 3A). Dead cells were excluded by gating on Sytox Blue-negative cells.

Statistical analysis

Statistical significance of differences between experimental groups was evaluated by a heteroscedastic, two-tailed

Student's *t*-test (corresponding to Welch's t-test) using Microsoft Excel (*$P<0.05$, **$P<0.01$, ***$P<0.001$).

Results

PARPi induce autophagy in parallel with cell death in ES cells

Since PARPi have been observed to induce autophagy in other tumours [39–41, 45], we initially tested whether PARPi would also induce autophagy in ES cells. To this end, we monitored the effect of two PARPi, olaparib and veliparib, on autophagy and cell death in two ES cell lines, WE-68 and SK-ES-1. Cells were exposed to PARPi for 48 h, and autophagy and cell death were assessed by flow cytometry. Autophagy was determined by Cyto-ID staining and cell death by PI uptake. Cyto-ID is a fluorescent dye that selectively labels autophagosomes [46–48], the key structures in the autophagic cascade [49]. Figure 1 shows that PARPi treatment induced cell death and autophagy in a concentration-dependent manner. Notably, the induction of cell death and autophagy followed the same pattern, with both drugs in both cell lines.

Linear regression analysis revealed a strong and statistically significant positive correlation between Cyto-ID fluorescence and PI uptake in both cell lines following PARP inhibition. This correlation was more pronounced in WE-68 cells (olaparib: $R^2 = 0.966$, $p<0.0001$; veliparib: $R^2 = 0.928$, $p<0.0001$) than in SK-ES-1 cells (olaparib: $R^2 = 0.733$, $p<0.001$; veliparib: $R^2 = 0.802$, $p<0.001$), suggesting a potentially cell line-dependent coupling between autophagy induction and cell death.

Similar to LC3 immunoblotting for the assessment of autophagy [50], Cyto-ID fluorescence alone is not sufficient to determine autophagic activity. However, the use of agents that block autophagosome turnover can provide evidence of changes in autophagy [50]. An additive or supra-additive effect of the combined treatment with the putative autophagy inducer and the autophagosome turnover blocker indicates enhanced autophagic activity. We therefore compared PARPi as single agents to PARPi in combination with the autophagosome turnover blocker CQ. The combination treatment resulted in a supra-additive effect compared to treatment with PARPi or CQ alone in WE-68 and SK-ES-1

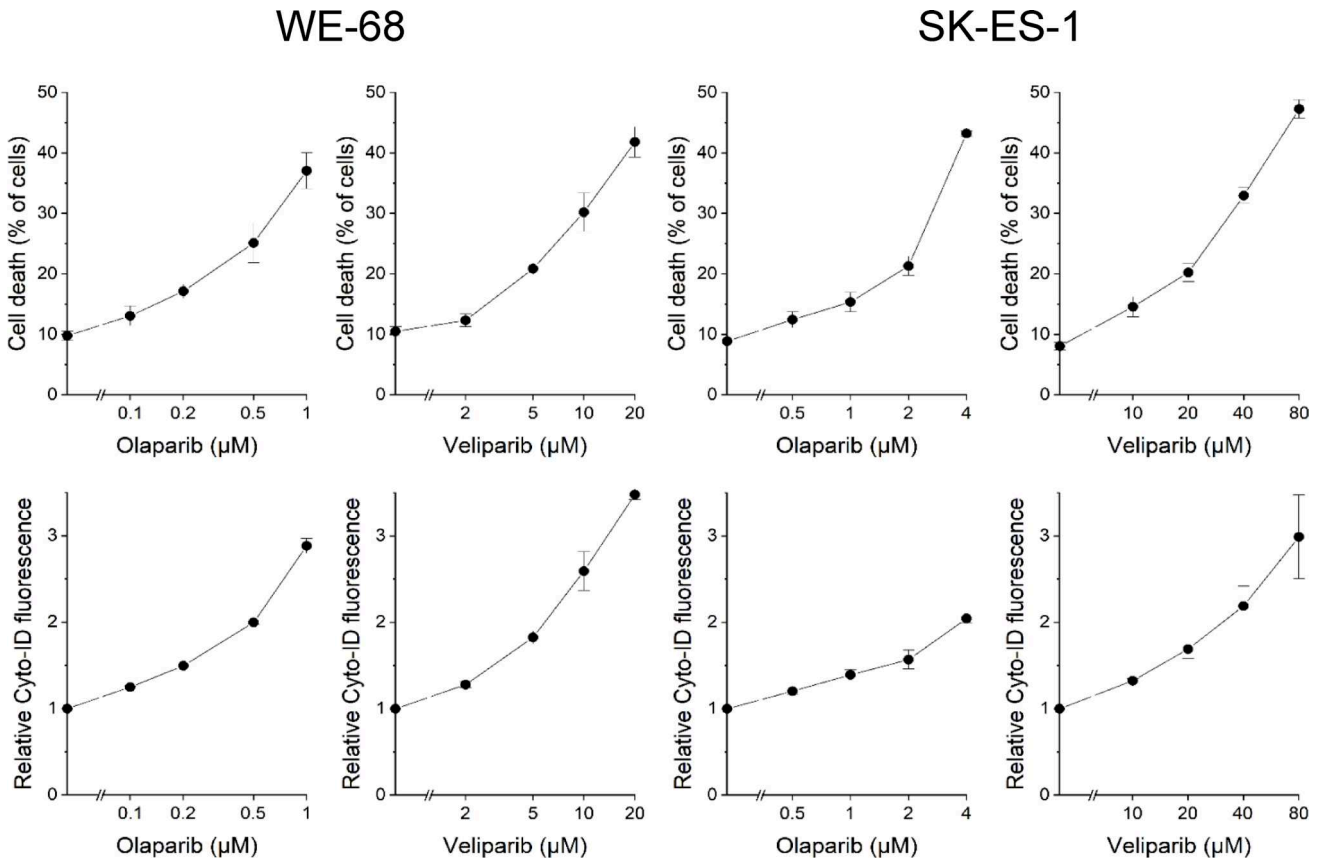


Fig. 1 PARPi induce cell death and autophagy in ES cells. Cells were exposed to PARPi for 48 h. Cell death and autophagy were determined by flow-cytometric analysis of PI uptake and Cyto-ID staining, respectively. Cyto-ID fluorescence intensities were normalised to the mean Cyto-ID fluorescence intensities of untreated cells. Means ± SEM of three biologically independent measurements are shown

cells (Fig. 2), evidencing that PARPi induced autophagy in ES cells.

PARPi induce greater cell death in cells with low autophagy than in cells with high autophagy

So far, our study has shown that PARPi induced autophagy in parallel with cell death in ES cells. To test whether autophagy indeed has an impact on PARPi-mediated cytotoxic effects, we utilised a recently developed Cyto-ID-based flow cytometric cell sorting method that separates cell populations into fractions with different basal autophagy levels, i.e., Aut^{LO}, Aut^{ME} and Aut^{HI} cell fractions, suitable for downstream culturing of sorted cells [44]. Figure 3A depicts the gating strategy used for cell sorting based on Cyto-ID staining, the aim of which was to generate subpopulations of similar cell number with different autophagic activities. When determining the persistence of the Aut^{LO}, Aut^{ME} and Aut^{HI} phenotypes, we observed that although the different autophagy levels tended to converge over time, they persisted for at least 6 h after sorting, and for 26 h in Aut^{HI} SK-ES-1 cells (Fig. 3B).

To assess whether autophagic activity could affect the cytotoxic effectiveness of PARPi, we treated the Cyto-ID-sorted cell fractions with olaparib or veliparib and subjected them to flow-cytometric analysis of cell death and $\Delta\psi_m$ loss after 48 h. Figure 4A shows that the Aut^{HI} fractions of both cell lines showed significantly less cell death than the Aut^{LO} fractions upon olaparib treatment. For example, olaparib killed up to 68.3% of Aut^{LO} WE-68 cells, but only up to 52.0% of Aut^{HI} WE-68 cells. In SK-ES-1 cells, olaparib-induced cell death reached 71.4% in the Aut^{LO} fraction and 52.6% in the Aut^{HI} fraction. In the Aut^{ME} fractions, olaparib-elicited cell death was intermediate between that in the Aut^{HI} and Aut^{LO} fractions, even though the differences did not reach statistical significance in all cases. Veliparib induced significantly higher cell death in the Aut^{LO} fraction compared to the Aut^{HI} fraction in SK-ES-1 cells, but not in WE-68 cells.

Loss of $\Delta\psi_m$ served as a second read-out to monitor the cytotoxic effectiveness of PARPi in cells with different autophagy levels. Figure 4B shows that the effects of PARPi on $\Delta\psi_m$ loss in Cyto-ID-sorted WE-68 and SK-ES-1 cells were consistent with those on cell death. Again, the Aut^{HI} fractions of both cell lines responded significantly less with loss of $\Delta\psi_m$ upon olaparib treatment than the Aut^{LO} fractions. In the case of veliparib, a significant difference between the Aut^{LO} and Aut^{HI} fractions was again observed only in SK-ES-1 cells.

Discussion

Preclinical studies indicate that PARPi offer a promising new therapeutic avenue for ES [19, 34, 51, 52]. However, translation of the preclinical findings to the clinic has not been crowned with success so far [24]. Therefore, the aim of current research is to identify the factors that determine PARPi resistance in ES to enable effective clinical use of this class of drugs [20]. Our study is the first to explore the impact of autophagy on the responsiveness of ES cells to PARPi.

In this study, we have found that PARPi promoted autophagy in parallel with cell death in ES cells. The induction of autophagy occurred at the same PARPi concentrations as the induction of cell death, suggesting that PARPi-mediated

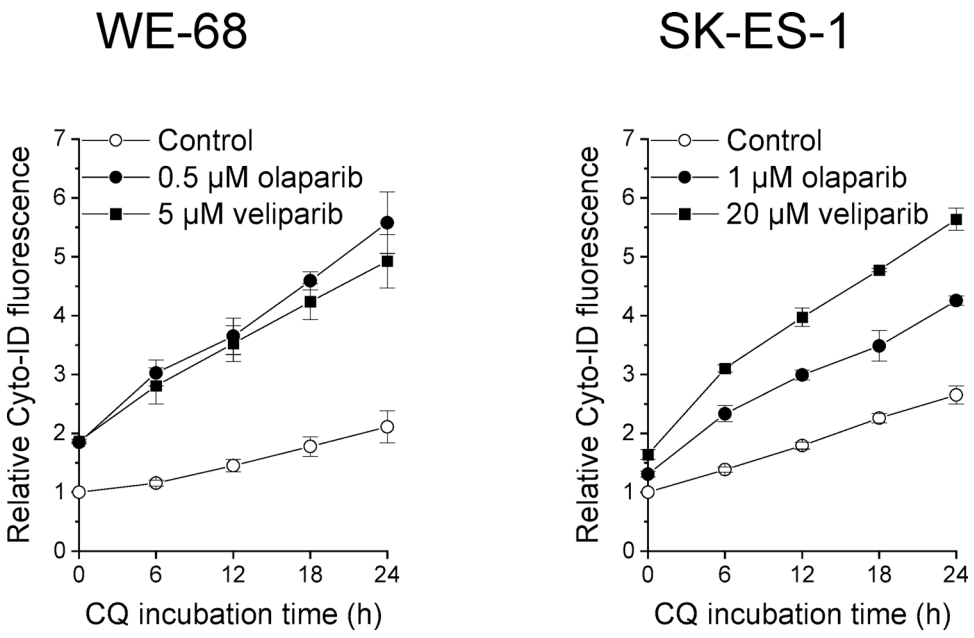
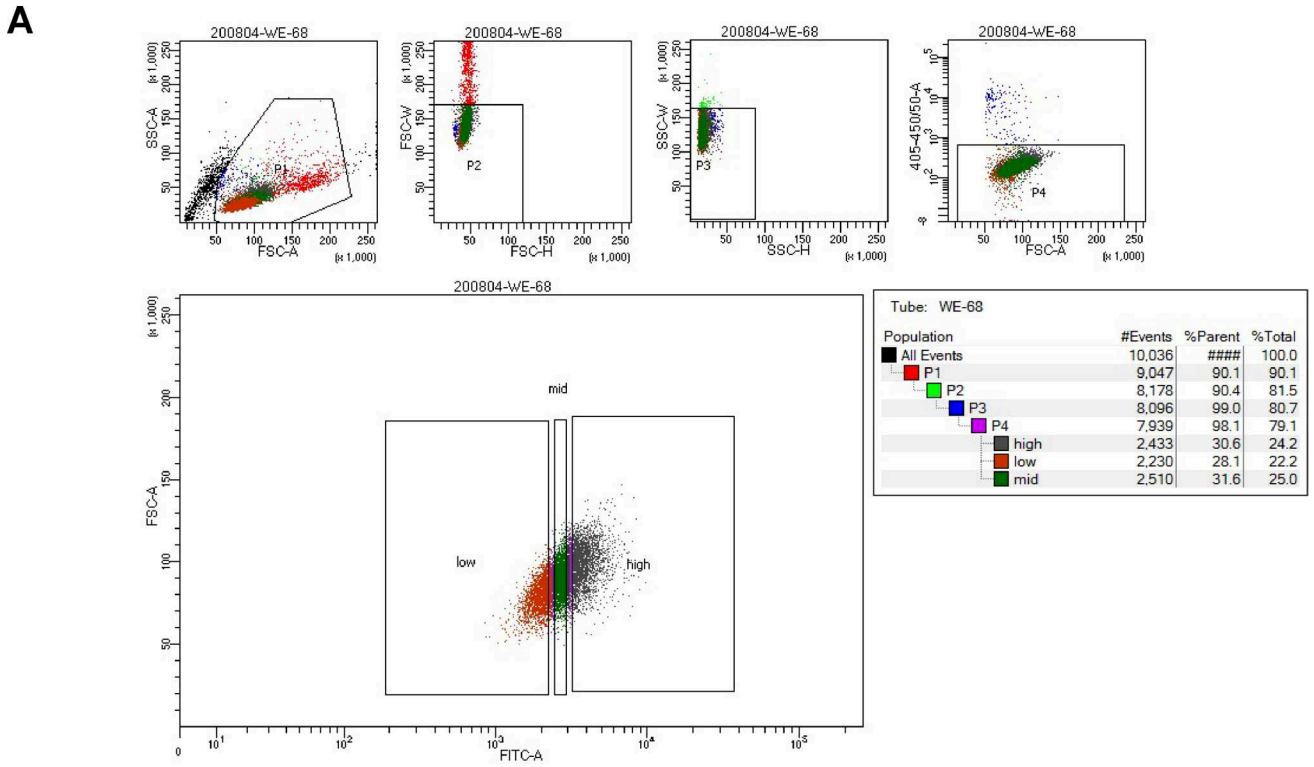


Fig. 2 CQ enhances PARPi-induced increase in Cyto-ID fluorescence intensity in ES cells. After a 24-h treatment with PARPi, cells were exposed to 25 µM CQ for the indicated times. Autophagy was determined by flow-cytometric analysis of Cyto-ID staining. Cyto-ID fluorescence intensities were normalised to the mean Cyto-ID fluorescence intensities of untreated cells. Means ± SEM of two biologically independent measurements are shown



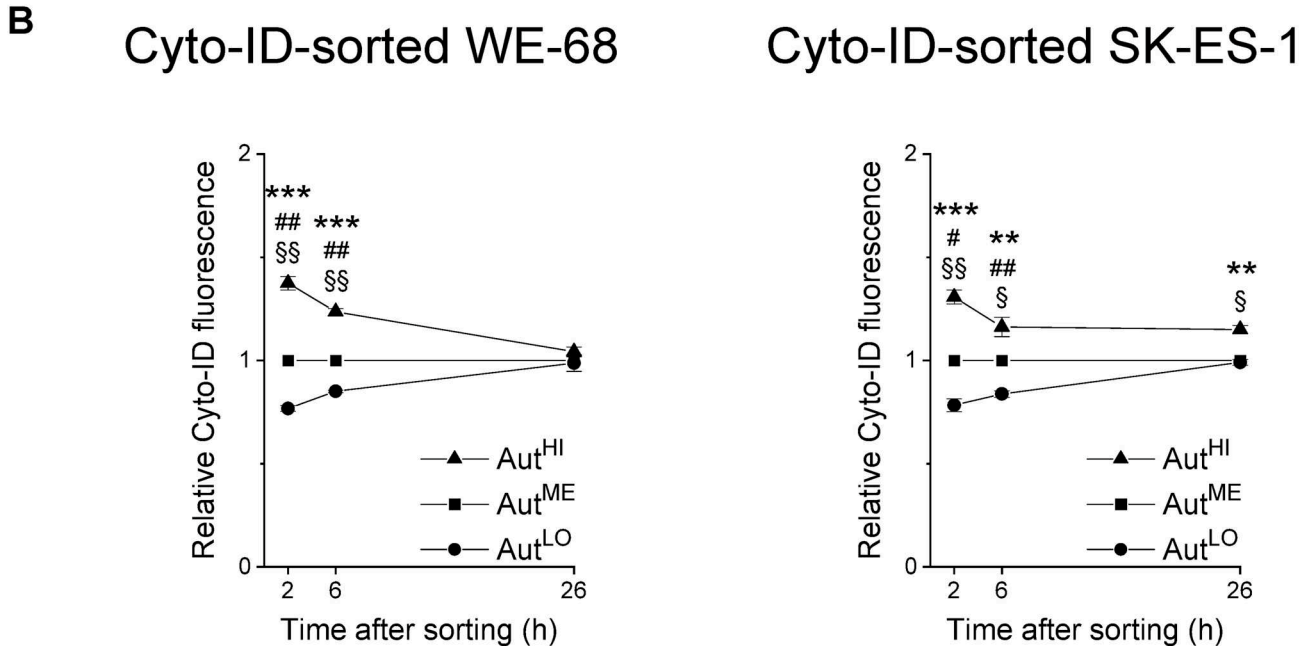


Fig. 3 Cyto-ID-based sorting of ES cells. (**A**) Debris and aggregates were excluded from cell sorting using a sequential gating strategy relying on FSC-A versus SSC-A followed by FSC-H versus FSC-W and SSC-H versus SSC-W. Dead cells were excluded by gating on Sytox Blue-negative cells. Cells were sorted into three subpopulations of approximately equal number based on their Cyto-ID fluorescence intensities, i.e., into Aut^{LO}, Aut^{ME} and Aut^{HI} subpopulations. (**B**) Cells were incubated for the indicated times after sorting, and autophagy was determined by flow-cytometric analysis of Cyto-ID staining. Cyto-ID fluorescence intensities of the three fractions were normalised to the Cyto-ID fluorescence intensity of Aut^{ME}. Means ± SEM of three biologically independent measurements are shown (Aut^{LO} vs. Aut^{HI}: $^{*}P<0.05$, $^{**}P<0.01$, $^{***}P<0.001$; Aut^{LO} vs. Aut^{ME}: $^{\#}P<0.05$, $^{\#\#}P<0.01$; Aut^{ME} vs. Aut^{HI}: $^{\S}P<0.05$, $^{\S\S}P<0.01$)

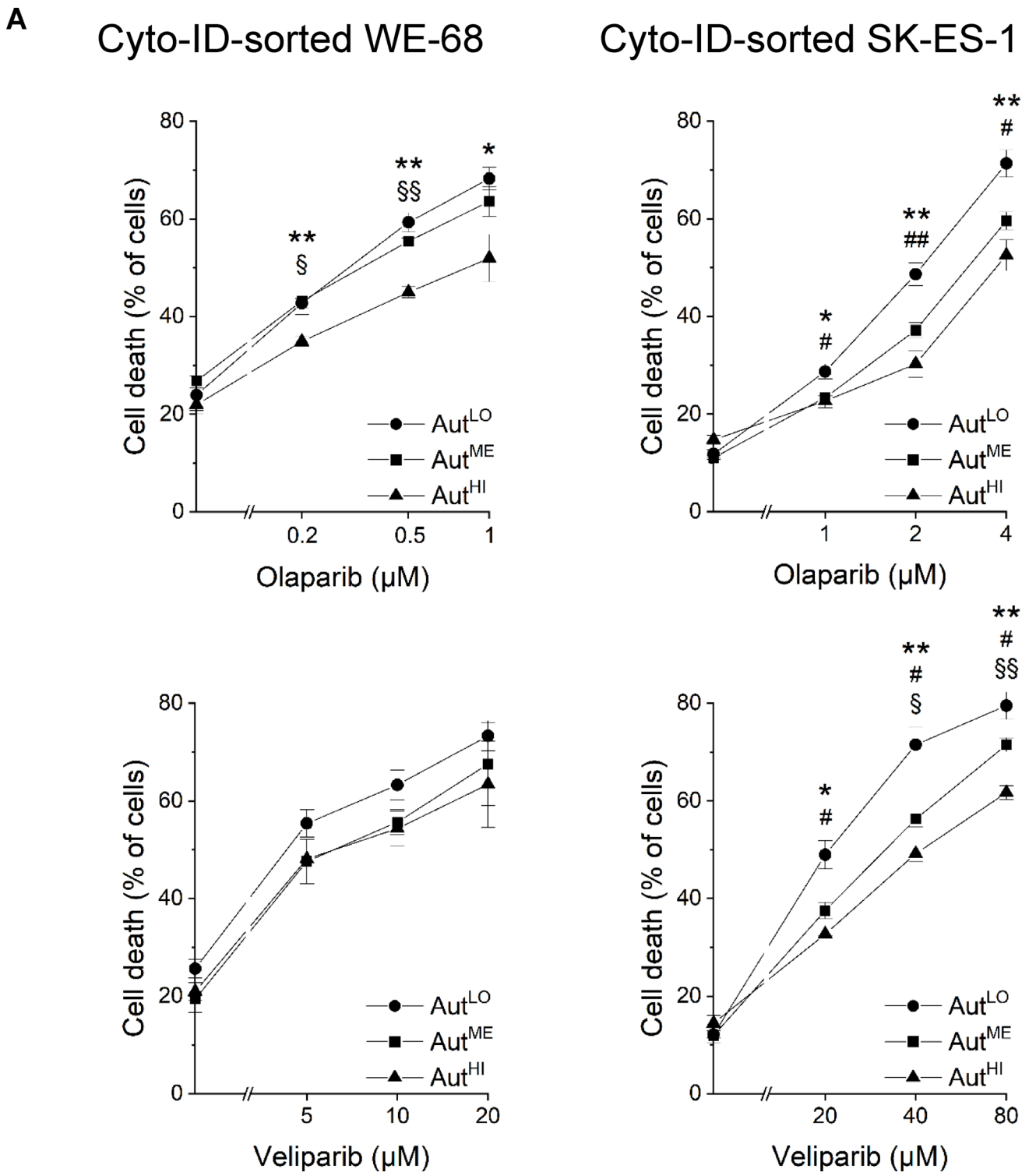


Fig. 4 ES cells with high autophagy are less sensitive to PARPi than ES cells with low autophagy. Cells were flow-cytometrically sorted based on their Cyto-ID fluorescence intensity into Aut^{LO}, Aut^{ME} and Aut^{HI} subpopulations. Two hours after sorting, cells were exposed to PARPi for 48 h. (**A**) Cell death and (**B**) loss of $\Delta\psi m$ were determined by flow-cytometric analysis of PI uptake and $DiIC_1(5)$ staining, respectively. Means ± SEM of three biologically independent measurements are shown (Aut^{LO} vs. Aut^{HI}: $^{*}P<0.05$, $^{**}P<0.01$; Aut^{LO} vs. Aut^{ME}: $^{\#}P<0.05$, $^{\#\#}P<0.01$; Aut^{ME} vs. Aut^{HI}: $^{\S}P<0.05$, $^{\S\S}P<0.01$)

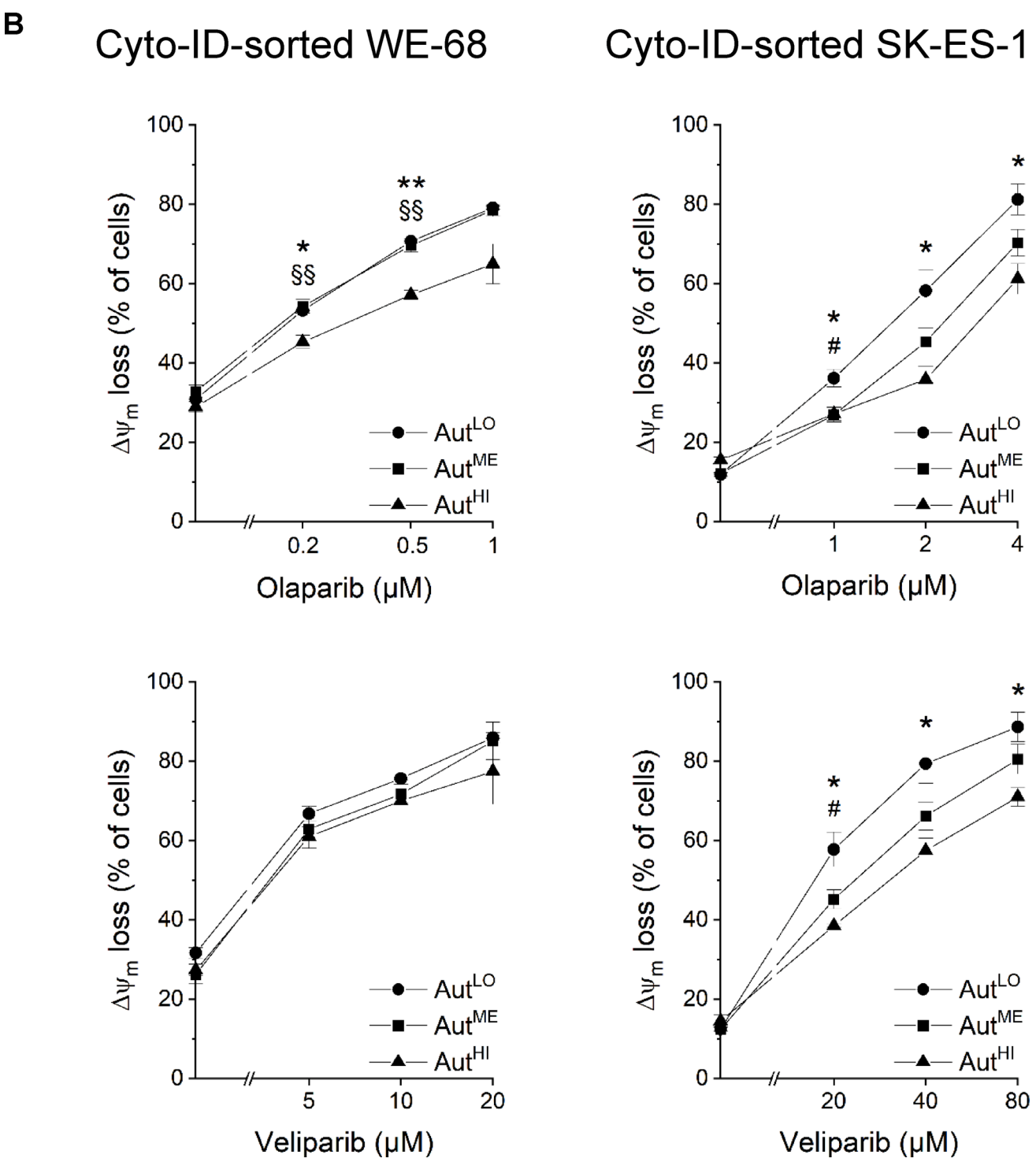


Fig. 4 (continued)

anticancer effects in ES cannot be achieved without concomitant activation of autophagy. It should be noted, however, that this does not necessarily imply a causal relationship between autophagy and cell death, but rather may suggest a pleiotropic effect of PARPi. In any case, PARPi may self-limit their anticancer effectiveness by inducing autophagy, as the latter plays a crucial role in the resistance of ES to antineoplastic drugs by acting as a survival mechanism under therapeutic stress [43]. To clarify whether autophagy is indeed a resistance mechanism to PARPi in ES, we compared the cytotoxic effectiveness of PARPi in ES cell populations with different autophagy levels. To this

end, we applied a method we recently developed to sort leukaemia cells according to their autophagic activity [44]. Our previous study demonstrated the suitability of Cyto-ID for autophagy-based cell sorting.

The results obtained from separating ES cell populations into subpopulations with different autophagy levels revealed a clear association between PARPi effectiveness and autophagy level in ES cells: they responded to PARPi in the order $Aut^{LO} > Aut^{ME} > Aut^{HI}$. It should in addition be taken into account that the differences in autophagy levels after sorting were transient, i.e., the autophagy in sorted cells persisted for at least 6 h after sorting but converged to baseline levels after 26 h in WE-68 cells. The results obtained may therefore even underestimate the actual effect of autophagy on PARPi effectiveness.

The transient nature of the differences in autophagy levels has another implication. EWS::FLI1 was shown to promote autophagy in ES cells by increasing the expression of ATG4B, a major regulator of the autophagic process [53]. Furthermore, a metabolism-associated gene signature, which includes autophagy-related genes, was developed for prognostic prediction in ES [54]. Similarly, the autophagy-related genes ATG2B, ATG10 and DAPK1 were found to have a potential protective function in ES [55]. It was thus concluded that the expression levels of autophagy-related genes may have prognostic value in ES. However, we observed a rapid reversion of the autophagy-sorted cell fractions, suggesting that the differences in autophagy levels were not due to genetic heterogeneity, but rather to stochastic fluctuations in autophagy activity in the initial cell population. A similar conclusion was reached in a study of autophagy-based sorted leukaemia cells, which showed that cell-to-cell differences in basal autophagy determined the apoptotic response to death ligands [56].

Conclusion

Autophagy plays a complex role in ES and can have both tumour-promoting and -suppressive functions, depending on the context [43]. This ambiguous role of autophagy in ES thus advises against its immediate targeting without further investigation. In any case, however, the results presented here suggest that basal autophagy levels may affect the efficacy of PARPi in patients with ES – with higher levels of autophagy being associated with decreased susceptibility to PARPi.

Acknowledgements Julia Clausen received a fellowship from the "IZKF des Universitätsklinikum Jena".

Author contributions The study conception and design were done by JC, TM, JFB and JS. Material preparation, data collection and analysis were performed by JC, DK, HMS, SB and JS. JS wrote the manuscript, and all authors commented on it. All authors approved the final manuscript.

Funding Open Access funding enabled and organized by Projekt DEAL. Julia Clausen received a fellowship from the "IZKF des Universitätsklinikum Jena".

Data availability The datasets analysed during the study are available from the corresponding author on reasonable request.

Declarations

Ethics approval Not applicable.

Competing interests The authors declare no competing interests.

Patient consent statement Not applicable.

Open Access This article is licensed under a Creative Commons Attribution 4.0 International License, which permits use, sharing, adaptation, distribution and reproduction in any medium or format, as long as you give appropriate credit to the original author(s) and the source, provide a link to the Creative Commons licence, and indicate if changes were made. The images or other third party material in this article are included in the article's Creative Commons licence, unless indicated otherwise in a credit line to the material. If material is not included in the article's Creative Commons licence and your intended use is not permitted by statutory regulation or exceeds the permitted use, you will need to obtain permission directly from the copyright holder. To view a copy of this licence, visit http://creativecommons.org/licenses/by/4.0/.

References

1. Grünewald TGP, Cidre-Aranaz F, Surdez D, Tomazou EM, de Álava E, Kovar H, Sorensen PH, Delattre O, Dirksen U (2018) Ewing sarcoma. Nat Rev Dis Primers 4(1):5
2. Riggi N, Suva ML, Stamenkovic I (2021) Ewing's sarcoma. N Engl J Med 384(2):154–164
3. Brennan B, Kirton L, Marec-Berard P, Gaspar N, Laurence V, Martin-Broto J, Sastre A, Gelderblom H, Owens C, Fenwick N et al (2022) Comparison of two chemotherapy regimens in patients with newly diagnosed Ewing sarcoma (EE2012): an open-label, randomised, phase 3 trial. Lancet 400(10362):1513–1521
4. Botta L, Gatta G, Capocaccia R, Stiller C, Canete A, Dal Maso L, Innos K, Mihor A, Erdmann F, Spix C et al (2022) Long-term survival and cure fraction estimates for childhood cancer in Europe (EUROCARE-6): results from a population-based study. Lancet Oncol 23(12):1525–1536
5. Delattre O, Zucman J, Plougastel B, Desmaze C, Melot T, Peter M, Kovar H, Joubert I, de Jong P, Rouleau G et al (1992) Gene fusion with an ETS DNA-binding domain caused by chromosome translocation in human tumours. Nature 359(6391):162–165
6. Knott MML, Hölting TLB, Ohmura S, Kirchner T, Cidre-Aranaz F, Grünewald TGP (2019) Targeting the undruggable: exploiting neomorphic features of fusion oncoproteins in childhood sarcomas for innovative therapies. Cancer Metastasis Rev 38(4):625–642
7. Flores G, Grohar PJ (2021) One oncogene, several vulnerabilities: EWS/FLI targeted therapies for Ewing sarcoma. J Bone Oncol 31:100404

8. Meyers PA, Federman N, Daw N, Anderson PM, Davis LE, Kim A, Macy ME, Pietrofeso A, Ratan R, Riedel RF et al (2024) Open-label, multicenter, phase I/II, first-in-human trial of TK216: a first-generation EWS::FLI1 fusion protein antagonist in Ewing sarcoma. J Clin Oncol 42(31):3725–3734
9. Gorthi A, Romero JC, Loranc E, Cao L, Lawrence LA, Goodale E, Iniguez AB, Bernard X, Masamsetti VP, Roston S et al (2018) EWS-FLI1 increases transcription to cause R-loops and block BRCA1 repair in Ewing sarcoma. Nature 555(7696):387–391
10. Keller KM, Krausert S, Gopisetty A, Luedtke D, Koster J, Schubert NA, Rodriguez A, van Hooff SR, Stichel D, Dolman MEM et al (2022) Target Actionability Review: a systematic evaluation of replication stress as a therapeutic target for paediatric solid malignancies. Eur J Cancer 162:107–117
11. Pearson ADJ, Federico S, Gatz SA, Ortiz M, Lesa G, Scobie N, Gounaris I, Weiner SL, Weigel B, Unger TJ et al (2023) Paediatric Strategy Forum for medicinal product development of DNA damage response pathway inhibitors in children and adolescents with cancer: ACCELERATE in collaboration with the European Medicines Agency with participation of the Food and Drug Administration. Eur J Cancer 190:112950
12. Zhao SJ, Prior D, Heske CM, Vasquez JC (2024) Therapeutic targeting of DNA repair pathways in pediatric extracranial solid tumors: current state and implications for immunotherapy. Cancers (Basel) 16(9):1648
13. Koppenhafer SL, Goss KL, Terry WW, Gordon DJ (2020) Inhibition of the ATR-CHK1 pathway in Ewing sarcoma cells causes DNA damage and apoptosis via the CDK2-mediated degradation of RRM2. Mol Cancer Res 18(1):91–104
14. Marx C, Schaarschmidt MU, Kirkpatrick J, Marx-Blümel L, Halilovic M, Westermann M, Hoelzer D, Meyer FB, Geng Y, Buder K et al (2021) Cooperative treatment effectiveness of ATR and HSP90 inhibition in Ewing's sarcoma cells. Cell Biosci 11(1):57
15. Martin JC, Sims JR, Gupta A, Hagoel TJ, Gao L, Lynch ML, Woloszynska A, Melendy T, Kane JF, Kuechle J, Ohm JE (2022) CDC7 kinase (DDK) inhibition disrupts DNA replication leading to mitotic catastrophe in Ewing sarcoma. Cell Death Discov 8(1):85
16. Sturm MJ, Henao-Restrepo JA, Becker S, Proquitté H, Beck JF, Sonnemann J (2023) Synergistic anticancer activity of combined ATR and ribonucleotide reductase inhibition in Ewing's sarcoma cells. J Cancer Res Clin Oncol 149(11):8605–8617
17. Collins VJ, Ludwig KR, Nelson AE, Sundara Rajan S, Yeung C, Vulikh K, Isanogle KA, Mendoza A, Difilippantonio S, Karim BO et al (2024) Enhancing standard of care chemotherapy efficacy using DNA-dependent protein kinase (DNA-PK) inhibition in preclinical models of Ewing sarcoma. Mol Cancer Ther 23(8):1109–1123
18. Ziener J, Henao-Restrepo JA, Leonhardi J, Sturm MJ, Becker S, Morales-Prieto DM, Milde T, Beck JF, Sonnemann J (2025) Combined inhibition of ribonucleotide reductase and WEE1 induces synergistic anticancer activity in Ewing's sarcoma cells. BMC Cancer 25(1):277
19. Vormoor B, Curtin NJ (2014) Poly(ADP-ribose) polymerase inhibitors in Ewing sarcoma. Curr Opin Oncol 26(4):428–433
20. Keller KM, Koetsier J, Schild L, Amo-Addae V, Eising S, van den Handel K, Ober K, Koopmans B, Essing A, van den Boogaard ML et al (2023) The potential of PARP as a therapeutic target across pediatric solid malignancies. BMC Cancer 23(1):310
21. Brenner JC, Feng FY, Han S, Patel S, Goyal SV, Bou-Maroun LM, Liu M, Lonigro R, Prensner JR, Tomlins SA, Chinnaiyan AM (2012) PARP-1 inhibition as a targeted strategy to treat Ewing's sarcoma. Cancer Res 72(7):1608–1613
22. Garnett MJ, Edelman EJ, Heidorn SJ, Greenman CD, Dastur A, Lau KW, Greninger P, Thompson IR, Luo X, Soares J et al (2012) Systematic identification of genomic markers of drug sensitivity in cancer cells. Nature 483(7391):570–575
23. Stewart E, Goshorn R, Bradley C, Griffiths LM, Benavente C, Twarog NR, Miller GM, Caufield W, Freeman BB 3rd, Bahrami A et al (2014) Targeting the DNA repair pathway in Ewing sarcoma. Cell Rep 9(3):829–841
24. Choy E, Butrynski JE, Harmon DC, Morgan JA, George S, Wagner AJ, D'Adamo D, Cote GM, Flamand Y, Benes CH et al (2014) Phase II study of olaparib in patients with refractory Ewing sarcoma following failure of standard chemotherapy. BMC Cancer 14:813
25. Dias MP, Moser SC, Ganesan S, Jonkers J (2021) Understanding and overcoming resistance to PARP inhibitors in cancer therapy. Nat Rev Clin Oncol 18(12):773–791
26. Bhamidipati D, Haro-Silerio JI, Yap TA, Ngoi N (2023) PARP inhibitors: enhancing efficacy through rational combinations. Br J Cancer 129(6):904–916
27. Li X, Zou L (2024) BRCAness, DNA gaps, and gain and loss of PARP inhibitor-induced synthetic lethality. J Clin Invest 134(14):e181062
28. Norris RE, Adamson PC, Nguyen VT, Fox E (2014) Preclinical evaluation of the PARP inhibitor, olaparib, in combination with cytotoxic chemotherapy in pediatric solid tumors. Pediatr Blood Cancer 61(1):145–150
29. Engert F, Schneider C, Weiß LM, Probst M, Fulda S (2015) PARP inhibitors sensitize Ewing sarcoma cells to temozolomide-induced apoptosis via the mitochondrial pathway. Mol Cancer Ther 14(12):2818–2830
30. Gill SJ, Travers J, Pshenichnaya I, Kogera FA, Barthorpe S, Mironenko T, Richardson L, Benes CH, Stratton MR, McDermott U et al (2015) Combinations of PARP inhibitors with temozolomide drive PARP1 trapping and apoptosis in Ewing's sarcoma. PLoS ONE 10(10):e0140988
31. Schafer ES, Rau RE, Berg SL, Liu X, Minard CG, Bishop AJR, Romero JC, Hicks MJ, Nelson MD Jr., Voss S et al (2020) Phase 1/2 trial of talazoparib in combination with temozolomide in children and adolescents with refractory/recurrent solid tumors including Ewing sarcoma: A Children's Oncology Group Phase 1 Consortium study (ADVL1411). Pediatr Blood Cancer 67(2):e28073
32. Chugh R, Ballman KV, Helman LJ, Patel S, Whelan JS, Widemann B, Lu Y, Hawkins DS, Mascarenhas L, Glod JW et al (2021) SARC025 arms 1 and 2: A phase 1 study of the poly(ADP-ribose) polymerase inhibitor niraparib with temozolomide or irinotecan in patients with advanced Ewing sarcoma. Cancer 127(8):1301–1310
33. Federico SM, Pappo AS, Sahr N, Sykes A, Campagne O, Stewart CF, Clay MR, Bahrami A, McCarville MB, Kaste SC et al (2020) A phase I trial of talazoparib and irinotecan with and without temozolomide in children and young adults with recurrent or refractory solid malignancies. Eur J Cancer 137:204–213
34. Strauss SJ, Berlanga P, McCabe MG (2024) Emerging therapies in Ewing sarcoma. Curr Opin Oncol 36(4):297–304
35. Mizushima N, Levine B (2020) Autophagy in human diseases. N Engl J Med 383(16):1564–1576
36. Jain V, Singh MP, Amaravadi RK (2023) Recent advances in targeting autophagy in cancer. Trends Pharmacol Sci 44(5):290–302
37. Qin Y, Ashrafizadeh M, Mongiardini V, Grimaldi B, Crea F, Rietdorf K, Gyorffy B, Klionsky DJ, Ren J, Zhang W, Zhang X (2023) Autophagy and cancer drug resistance in dialogue: pre-clinical and clinical evidence. Cancer Lett 570:216307
38. Elshazly AM, Nguyen TVV, Gewirtz DA (2022) Is autophagy induction by PARP inhibitors a target for therapeutic benefit? Oncol Res 30(1):1–12
39. Santiago-O'Farrill JM, Weroha SJ, Hou X, Oberg AL, Heinzen EP, Maurer MJ, Pang L, Rask P, Amaravadi RK, Becker SE et

al (2020) Poly(adenosine diphosphate ribose) polymerase inhibitors induce autophagy-mediated drug resistance in ovarian cancer cells, xenografts, and patient-derived xenograft models. Cancer 126(4):894–907
40. Zai W, Chen W, Han Y, Wu Z, Fan J, Zhang X, Luan J, Tang S, Jin X, Fu X et al (2020) Targeting PARP and autophagy evoked synergistic lethality in hepatocellular carcinoma. Carcinogenesis 41(3):345–357
41. Pai Bellare G, Saha B, Patro BS (2021) Targeting autophagy reverses de novo resistance in homologous recombination repair proficient breast cancers to PARP inhibition. Br J Cancer 124(7):1260–1274
42. Cahuzac M, Langlois P, Peant B, Fleury H, Mes-Masson AM, Saad F (2022) Pre-activation of autophagy impacts response to olaparib in prostate cancer cells. Commun Biol 5(1):251
43. Koustas E, Sarantis P, Karamouzis MV, Vielh P, Theocharis S (2021) The controversial role of autophagy in Ewing sarcoma pathogenesis-current treatment options. Biomolecules 11(3):355
44. Gschwind A, Marx C, Just MD, Severin P, Behring H, Marx-Blümel L, Becker S, Rothenburger L, Förster M, Beck JF, Sonnemann J (2022) Tight association of autophagy and cell cycle in leukemia cells. Cell Mol Biol Lett 27(1):32
45. Arun B, Akar U, Gutierrez-Barrera AM, Hortobagyi GN, Ozpolat B (2015) The PARP inhibitor AZD2281 (Olaparib) induces autophagy/mitophagy in BRCA1 and BRCA2 mutant breast cancer cells. Int J Oncol 47(1):262–268
46. Chan LL, Shen D, Wilkinson AR, Patton W, Lai N, Chan E, Kuksin D, Lin B, Qiu J (2012) A novel image-based cytometry method for autophagy detection in living cells. Autophagy 8(9):1371–1382
47. Oeste CL, Seco E, Patton WF, Boya P, Perez-Sala D (2013) Interactions between autophagic and endo-lysosomal markers in endothelial cells. Histochem Cell Biol 139(5):659–670
48. Guo S, Liang Y, Murphy SF, Huang A, Shen H, Kelly DF, Sobrado P, Sheng Z (2015) A rapid and high content assay that measures cyto-ID-stained autophagic compartments and estimates autophagy flux with potential clinical applications. Autophagy 11(3):560–572
49. Melia TJ, Lystad AH, Simonsen A (2020) Autophagosome biogenesis: from membrane growth to closure. J Cell Biol 219(6):e202002085
50. Mizushima N, Yoshimori T, Levine B (2010) Methods in mammalian autophagy research. Cell 140(3):313–326
51. Caltavituro A, Buonaiuto R, Pietroluongo E, Morra R, Salomone F, De Placido P, Pagliuca M, Vaia A, Ottaviano M, Tortora M et al (2023) Shifting from a biological-agnostic approach to a molecular-driven strategy in rare cancers: Ewing sarcoma archetype. Biomedicines 11(3):874
52. Jia K, Cao L, Yu Y, Jing D, Wu W, Van Tine BA, Shao Z (2025) Signaling pathways and targeted therapies in Ewing sarcoma. Pharmacol Ther 266:108765
53. Lu Q, Zhang Y, Ma L, Li D, Li M, Li J, Liu P (2017) EWS-FLI1 positively regulates autophagy by increasing ATG4B expression in Ewing sarcoma cells. Int J Mol Med 40(4):1217–1225
54. Chen ZY, Yang H, Bu J, Chen Q, Yang Z, Li H (2021) Prognosis implication of a novel metabolism-related gene signature in Ewing sarcoma. J Oncol 2021:3578949
55. Wen J, Wan L, Dong X (2022) The prognostic value of autophagy related genes with potential protective function in Ewing sarcoma. BMC Bioinformatics 23(1):306
56. Gump JM, Staskiewicz L, Morgan MJ, Bamberg A, Riches DW, Thorburn A (2014) Autophagy variation within a cell population determines cell fate through selective degradation of Fap-1. Nat Cell Biol 16(1):47–54

Publisher's note Springer Nature remains neutral with regard to jurisdictional claims in published maps and institutional affiliations.